Propellants, Explosives, Pyrotechnics

Investigation of Energetic Particle Distribution from High-Order Detonations of Munitions

Michael R. Walsh,*[a] Tracey Temple,[b] Matthew F. Bigl,[a] Seipati F. Tshabalala,[b] Nathalie Mai,[b] and Melissa Ladyman[b]

Abstract: Military training with munitions containing explosives will result in the deposition of energetic materials on ranges. These residues contain compounds that may result in human health impacts when off-range migration occurs. Models exist that predict the spatial and mass distribution of particles, but they have proven to be difficult to apply to detonating munitions. We have conducted a series of tests to determine if modelling results can be directly applied to simple detonation scenarios. We also command detonated several rounds to obtain an initial indication of high-order detonation particle distributional heterogeneity.

The detonation tests indicate that particle distributions will be quite heterogeneous and that the model used did not adequately describe the distribution of detonation residues. This research will need to be expanded to build an empirical database sufficient to enable the refinement of existing models and improve their predictions. Research on low-order detonations should be conducted as low-order detonations will result in higher mass deposition than high-order detonations. Distribution models verified with empirical data may then be incorporated into range management models.

Keywords: Munitions Residue · High-order Detonation · Particle Spatial Distribution · Mass Distribution · Modelling

1 Introduction

Training with live munitions is an integral part of military preparedness. Any munition that is fired contains energetic materials such as propellants, explosives, or incendiaries. The compounds that make up these energetic materials can be found on training ranges [1–4]. Evidence includes energetics in soil and water samples taken from active and legacy ranges and the impacts to wildlife and vegetation on training ranges [5–8]. Many energetic compounds are water-soluble and will migrate to groundwater, enabling transport off range, compromising drinking water resources, and threatening human health and range sustainability [9–12].

Energetics residues have varying effects on the environment, based in large part upon their component toxicity, compound dissolution rates in water, and the ability of the environment to transform or attenuate the transport of potentially toxic compounds. Internationally, a new class of ordnance called insensitive munitions (IM) is being certified for use on training ranges. Some of these munitions contain highly soluble compounds in their insensitive high-explosive (IHE) formulations [13–16]. Up to 99% of compounds such as ammonium perchlorate (AP), Nitrotriazolone (NTO), and Nitroguanidine (NQ) will dissolve out of the high-order detonation residues upon exposure to liquid water [17]. Immediate dissolution of energetics constituents from detonation residues may result in a high-concentration mass of energetics migrating through the soil column that may overcome the ecosystem's ability to react to the compounds. The impacts that energetics formulations and their constituent compounds will have on range sustainability is currently being studied [18].

To prevent adverse consequences, several models have been developed to predict the impact that training with live munitions will have on military ranges [19–22]. In addition, empirical data is available on the mass of energetics resulting from the firing and detonation of munitions [23, 24]. These data include some spatial information in the form of the overall residues deposition area. Particle size distribution data is also available for several munitions that detonated low-order or resulted from inefficient blow-in-place (BIP) tests (Table 1) [10, 13, 25]. What is not available is sufficient empirical data on the physical characteristics and spatial distribution of residues to refine existing models so that they can be used to effectively predict the spatial distribution of particles from detonations [19].

Analysis of current particle dispersion models indicates that they are based on a near-uniform spatial distribution of residues based on an assumed particle size distribution

[a] M. R. Walsh, M. F. Bigl
US Army Cold Regions Research and Engineering Laboratory
72 Lyme Road
Hanover, New Hampshire 03755 USA
*e-mail: Michael.Walsh@usace.army.mil
[b] T. Temple, S. F. Tshabalala, N. Mai, M. Ladyman
Center for Defence Chemistry
Cranfield University
Defence Academy of the UK
SN6 8LA

These are not the final page numbers! ↗↗

Full Paper

M. R. Walsh, T. Temple, M. F. Bigl, S. F. Tshabalala, N. Mai, M. Ladyman

Table 1. Detonation Characteristics Descriptors

Descriptor	Filler Mass Consumed	Munition State
High-order detonation (HI)	99.99 % or more	Total fragmentation of projectile body. Very fine residues (soot).
Low-order detonation (LO)	75 % to 99.98 %	Incomplete body fragmentation. Energetics particles on the ground and adhered to larger metal fragments.
Partial detonation	25 % to 75 %	Little if any fragmentation of the body. Large chunks of explosive filler (>cm size).
Initiated dud	<25 %	Fuze initiated. Mostly intact round. Adjacent loose chunks of explosive filler possible.
Non-initiated dud	None	Round intact, including fuze. No ejection of explosive filler.

[2, 26]. For high-order detonations of munitions, there are no empirical data in the literature to confirm the assumption of uniform particle distribution. Research on mass deposition of energetic residues from high-order detonations indicates that residues tend to be very fine and to form near-annular dispersion patterns in low-wind situations (Figure 1) [27]. Very limited spatial distribution data are available from these tests, mostly in the form of overall energetics deposition area. We have also found that low-order detonations make up a small percentage of munitions detonations but are the dominant source of energetics mass on ranges [28,29]. Low-order detonation residues spatial distribution, which must also be considered in particle dispersion models, will be examined in a future paper.
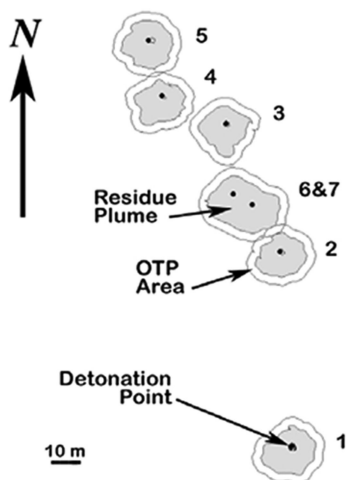

Figure 1. Residue deposition areas.

There is a tendency to tie explosives residues dispersion to metal fragmentation (frag) dispersal, which is only appli-

cable if the residues are adhered to the frag [30,31]. This occurs primarily with detonations that are less efficient than high-order detonations, as frag for high-order detonations tends to be much smaller and initially at higher temperatures, resulting in very little energetics adhesion. Models that take into account particle dispersion based on size and mass have used simulated or very limited empirical data [2] [19] [32].

Additional empirical data for spatial distribution of energetics from high-order detonations of munitions are needed to better refine existing dispersion models. The objective of the work presented in this paper was to conduct preliminary research to determine if spatial data for high order detonations could be collected and if the data conform to the model predictions.

2 Experimental Section

We used three methods to investigate post high-order detonation explosive particle spatial distribution. In the first phase of the study, we examined past high-order detonation tests to derive a method to use the available data to estimate gross particle distribution. In the second phase, we conducted high-order detonation tests on clean ice and measured the physical and spatial characteristics of the particles. In the third phase, we used a computational modeling tool, Propagation of Shock in Air (ProSAir [33]), to determine how far energetics residues from a specific charge size would travel in the environment. Phase 3 experiments were undertaken under controlled conditions to minimize the impact of environmental variables such as wind on dispersion [33].

Phase 1: High-order Detonation General Dispersion Patterns

High-order detonation tests have been conducted on snow for many years to estimate energetics residues mass resulting from training with live munitions [34,35]. The basis for these tests is to collect a representative sample of the deposition area and calculate the mass of energetics residues within that area. Replicate sampling and quality assurance procedures are conducted to determine the robustness of the data. Data from tests conducted in January of 2004 to characterize the distribution of residues from within demarcated live-fire detonation deposition areas were re-examined to determine if a rough correlation between distance from the detonation point or perceived density of the residues on snow can be made with the actual residues distribution [36]. These factors were then applied to the deposition area to determine if this correlation may be useful to models. No quantitative measurements of particle sizes were conducted during testing, only the mass of energetics within each area or sub-area sampled was measured.

⤣⤣ These are not the final page numbers!

Phase 2: Spatial Distributions from Detonated Rounds

The spatial distribution of explosives residues particles from the detonation of munitions in the field was tested in March of 2015 on the Eagle River Flats impact range on Joint Base Elmendorf-Richardson in Alaska. At the time of the tests, the range was covered with a moderate layer of ice (30 cm) and was free of snow. Low ambient temperatures ($\approx -20\,°C$) resulted in a dry ice surface, ideal for particle collection. For these tests, we used 81-mm mortar rounds containing a multi-component insensitive high-explosive filler containing RDX, Dinitroanisole (DNAN), and NTO. All rounds were command detonated using a fuzing system designed by the Cold Regions Research and Engineering Laboratory (CRREL) that contained a Composition C-4 booster pellet (97% RDX). Initiation was through a blasting cap inserted in the nose of the fuze. The detonation thus occurred in a fully enclosed round (Figure 2).

Figure 2. Fuzing for Phase 2 command detonation tests.

Three test locations were set up on the ice at the Flats. At each location, a center detonation point was marked and concentric circles 1-m in width out to 10-m from the detonation point were demarcated. Aluminum pie pans (20 cm) were screwed to the ice radially from the central detonation point (Figure 3). Distances between detonation points were
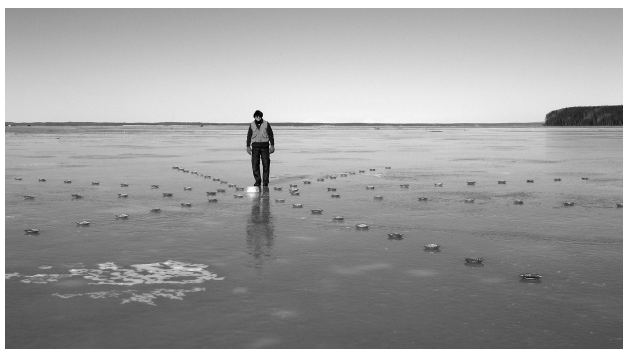

Figure 3. Detonation residues collection pans on ice surface for Phase 2 tests.

based on high-order detonation plume sizes established during prior field-testing of 81-mm mortar rounds [15].

Rounds were detonated with the objective of attaining a high-order detonation. All rounds for these tests had the tail assemblies removed and the body of the round mounted vertically on an aluminum plate. We characterized the detonation based on post-detonation energetics residues. We use this quantification method rather than a qualitative assessment method such as those described in NATO STANAG AOP-39 and MIL-STD-2105 because it yields quantitative data that can be validated through quality assurance methods [37,38]. The characterization measurement is based on the percent of explosive filler consumed during the detonation (Table 1). Note that the descriptor considers the filler as a whole. One of the advantages of the characterization method used in this study is that the method allows the analysis of the residues for the various constituents that make up the energetic filler. It is thus possible to determine detonation efficiencies for energetic compounds as well as the filler as a whole.

The fuzes contained 18 g of C4 explosive to trigger the desired detonation type (HO). Initiation was by detonation cord and time fuze. As these were the first tests of this type conducted involving spatial distribution, we collected samples in a variety of ways to determine how best to sample for the data needed. For high-order detonations, we were interested in both particle size and total residues mass, which we later compared to high-order residues masses from other types of sample collections [36]. Thus, particles were collected in aluminum pans screwed into the ice to investigate the particle-size to spatial-distribution relationship, and the remaining visible residues were swept up to get a mass balance of the energetics following detonation (Table 2).

Table 2. Sample Collection Methods for Phase 2 Tests

Test	Sample Collection Methods
HI-1	Collected particles from pans
	Swept up remaining residues for analysis
HI-2	Collected particles from pans
HI-3	Swept up all detonation residues for analysis

The high-order particle distribution samples, which also contained ice particles and detonation debris, were returned frozen to the CRREL analytical lab in Hanover, NH, for processing and measurement. The particles were freeze-dried to remove any ice. The remaining particles were sieved and examined microscopically to roughly determine size distributions. Some particle differentiation was possible based on coloration, the crystals of explosives appearing dull white under a microscope. The swept residues that were collected for the overall energetic residues mass estimation were melted ($4\,°C$), vacuum filtered, and analyzed using methods developed by Walsh [39,41].

These are not the final page numbers! ↗↗

Phase 3: Unconfined Charge Distribution Tests

The Phase 3 unconfined detonation particle distribution tests were conducted in a large open-ended steel container to minimize environmental variables. The ISO shipping container used for the tests measured approximately $6 \times 2.4 \times 2.5$ m. One end of the container (2.4×2.5 m) was left open during testing.

The ProSAir [33] computational tool was used to predict the maximum energetics mass for the tests by estimating the residues travel distance for a given unconfined explosive mass detonation within the ISO container. A steel witness plates used to collect the explosive residue was designed based on the ProSAir particle dispersal estimate (Figure 4a). For the ISO container, the ProSAir tool recommended up to 5-g of unconfined plastic explosive PE7 (88 % RDX, 12 % binder) and steel witness plates 2 m in diameter. Charges of 2.5 g and 5 g were used for the experiments. The circular witness plate was divided into four quadrants; one quadrant was further sub-divided into 15 radial removable particle collection segments. The PE7 charges were hand-molded into spherical charges and a No. 8 Detonator (0.75-g penta-erythritol tetranitrate (PETN)) was used as a booster to the main charge to ensure high order detonation. The detonator was placed in the center of the charge, which was suspended at a height of 0.5 m above the center of the witness plate. The area inside the container was prepared by hanging cotton sheets over the three surrounding walls and the ceiling to capture any residue that may travel beyond the predicted distance. The steel witness plates were then placed in position. The steel witness plates were cleaned with acetone prior to each detonation.
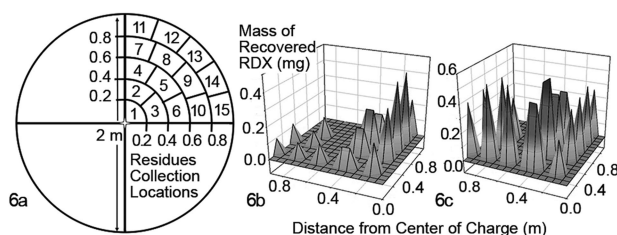
Figure 4. Phase 3 setup and results: a) Setup of steel witness plate, b) 2.5 g Charge deposition results, c) 5 g Charge deposition results.

Following charge detonation, the witness plates were swiped with cotton swabs dampened with acetone. The swabs were placed in airtight jars for transportation to the analytical lab, where the swabs were submerged in acetone. The jars were sonicated for 10 min and the swabs were rinsed with acetone and pressed tightly to remove the solvent. The acetone was evaporated to dryness under nitrogen gas flow and 50:50 acetonitrile:water was added to make up the volume to 10 mL. The solutions were filtered and aliquots were analyzed using HPLC. Analyses were undertaken using an Alliance series liquid chromatography-photodiode array (LC-PDA) detection system (Waters UK, Elstree, UK). Separation was carried out on an ACE UltraCore 2.6 μSuperPhenylHexyl column (4.6×100 mm) from Hichrom, Ltd, using a 40:60 acetonitrile:water mobile phase at a flow rate of 1 ml/min. The column was maintained at 30 °C and the injection volume was 10 μl. Detection was achieved at 210 nm. The method was linear over the concentration range of 1 to 50 ppm.

3 Results

Phase 1: High-order Detonation General Dispersion Patterns

High-order detonation energetics residues deposition areas for five common US munitions are presented in Table 3. We have separated the data by munition size and energetic filler. For data that have been reported earlier, a reference is given. The explosive formulations include Trinitrotoluene (TNT), Composition B (Comp-B: RDX/TNT), PAX-21 (RDX, DNAN, AP), and IMX-104 (DNAN, NTO, RDX). Chemical nomenclature are given in the List of Acronyms at the end of this paper.

There are differences in deposition areas within similar rounds and overlap between rounds of different sizes. The very small particle sizes of the high-order residues make them very susceptible to aerial transport. Variations in wind velocity will have a great effect on the residues dispersal pattern and the deposition area. In tests conducted with 81-mm IMX-104 rounds, the area of deposition for five simultaneously command detonated rounds varied from 580 to 890 m^2 [41]. Table 3 also contains high-order detonation residues dispersal patterns from fired 81mm and 105-mm Comp-B high-explosive rounds and 155-mm TNT and Comp-B rounds that were blown in place (BIP).

Post detonation residues on snow were sampled based on a subjective perceived deposition density gradient (dark/medium/light). There was no consistent correlation between the estimated mass of energetics recovered and the residues density for a fired 105-mm HE round and the two 155-mm BIP rounds (Table 4). The BIP detonations are used in this analysis because the efficiency of the detonation indicates a near-high-order detonation occurred during the operation. The complete deposition area was also sampled and an estimate for total residues mass was calculated as a quality assurance procedure for the test. In all three cases, the cumulative residues from the three density zones are within a factor of 2 of the estimates for the total deposition areas. The percent of residues in each of the three zones indicates that it is important that not just areas that are perceived as contaminated are sampled. The residues in "light" density zones, where there were only traces of residues on

These are not the final page numbers!

Table 3. Detonation Residues Deposition Areas

Munition	Explosive Formulation	Detonation Type	Number of Rounds	Deposition Area (m²)	Source
Mortar Rounds					
60-mm	Comp-B	Live-fire[a]	7	220	[23]
	PAX-21	Command[b]	7	330	[13]
	IMX-104	Command	7	250	[15]
81-mm	Comp-B	Live-fire	14	230	[23]
	IMX-104	Command	7	350	[15]
	IMX-104[c]	Command	5	670	[41]
	IMX-104	Command	2	460	
120-mm	Comp-B	Live-fire	8	450	[23]
Howitzer Rounds					
105-mm	Comp-B	Live-fire	13	530	[23]
155-mm	Comp-B	Live-Fire	7	940	[23]
	TNT	Live-fire	7	760	[23]

[a] Deposition from rounds fired into an impact area; [b] Deposition from static (command) detonated rounds using a fuze simulation system; [c] Fuze simulator booster mass increased 50% from previous test

Table 4. Gradient-based Energetics Residues Mass Distribution Tests[a] [36]

Test (Efficiency)	Zone Sampled[b]	Deposition Area (m²)	Residues Mass (mg)	Percent of Residues	Residues /Unit Area (mg/m²)
105-4: HI	All	810	21	–	0.024
(99.999%)	Dark	97	7.5	61%	0.077
	Medium	61	0.3	2%	0.004
	Light	650	4.4	37%	0.007
155-1: BIP	All	1200	16	–	0.013
(99.999%)	Dark	70	0.3	2%	0.004
	Medium	370	7.3	39%	0.021
	Light	840	11	59%	0.013
155-7: BIP	All	1200	18	–	0.015
(99.999%)	Dark	97	11	52%	0.110
	Medium	320	6.2	29%	0.019
	Light	770	3.9	19%	0.005

[a] Data derived from external donor charge BIP operations on single rounds; [b] Perceived density of residues on snow as determined by darkness of deposition

the snow surface, contributed significantly to the total mass estimate.

In the three tests for which deposition area samples were collected based on the radial distance from the detonation point (zonal-based measurements), there is an obvious correlation between distance and deposition. Results are consistent based on distance from the detonation point, with about an order of magnitude reduction in residues for each 10-m increase in distance from the detonation point (Table 5). There is very little difference among tests in both the estimated percent of residues and the density of those residues in each 10-m band extending out from the detonation point, even though the 81-mm round contained 950 g of Comp-B whereas the 105-mm round contained 2100 g of Comp-B explosive.

For the zonal tests, a 3-m annulus surrounding the visually demarcated residues deposition area was also sampled to determine if a significant amount of residues lay outside the perceived deposition area. The estimated average mass of energetic residues recovered in the 3-m annulus was <2% of the total estimated mass within the demarcated area, indicating that the deposition areas were correctly demarcated.

Phase 2: Spatial Distributions from Detonated Rounds

The shock wave and body fragmentation from the detonations of HI-1 and HI-2 resulted in a loss of several of the sampling pans set out to collect energetic particle residues. For HI-1, the rings of pans within 3 m of the detonation were destroyed, and for HI-2, the pans within the first two rings were missing. There was much debris associated with the initiation system (detonation cord, blasting cap, fuze simulator) mixed in with the energetics residues, making separation difficult. However, some particles were separated and photographed. An image of high-order detonation residues particles is shown in Figure 5. The particles in the im-

Table 5. Zonal-based Mass Distribution Tests (HO detonations) [36]

Test	Zone	Deposition Area (m²)	Est. Mass of Residues (mg)	Percent of Residues	[b]Residues Density (mg/m²)
81-5	< 10 m[a]	190	19	72%	0.100
	10–20 m	230	6.1	23%	0.027
	> 20 m	380	1.2	5%	0.003
105-3	< 10 m	280	27	83%	0.096
	10–20 m	390	4.6	14%	0.012
	> 20 m	260	0.8	3%	0.003
105-7	< 1 m	230	20	77%	0.087
	10–20 m	370	4.8	18%	0.013
	> 20 m	350	1.2	5%	0.003
Means	< 10 m	230	22	78%	0.096
(n = 3)	10–20 m	330	5.2	18%	0.016
	> 20 m	320	1.1	4%	0.003

[a] Annular distance from detonation point; [b] Perceived density of residues as determined by darkness of deposition
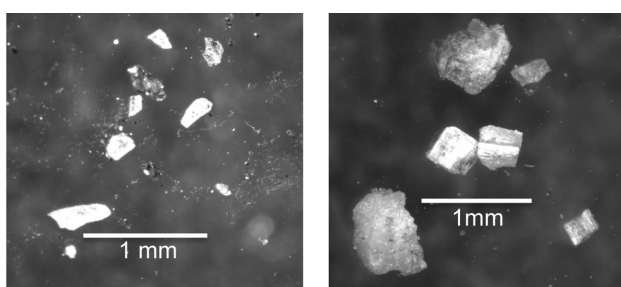

Figure 5. Photomicrograph of high-order (left) and low-order (right) post-detonation particles.

age are < 1 mm in their longest dimension. As distance increases from the detonation point, the number of particles decreases and the fine soot particles (< 0.25 mm) dominate (Table 6). Because of the very large number of smaller particles, a percentage of the total mass in the annulus is given rather than an estimate of the number of particles. The larger particles tend to be metallic fragments or debris from the initiation system with little evidence of energetics. The pattern distribution of energetics (mass) is illustrated in Figure 6 and shows a non-uniform distribution. The presence
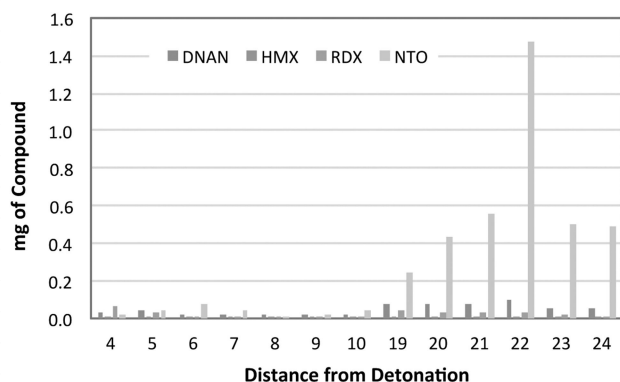
of elevated NTO beyond 20 m from the detonation point indicates the presence of undetonated crystals of the compound.

Analysis of the swept deposition areas of HI-1 and HI-3 confirm that energetics deposition is quite low, indicating detonations approaching high-order (Table 7). Data are compared with previous data obtained from similar command-detonation high-order tests with the same round but on snow-covered ice (n = 7). RDX and DNAN sample concentrations were at or just above analytical instrumentation detection limits, leading to some variability between samples. The percent values below the mass values for each component is the percent of that component recovered as compared to the original mass of that component in the test configuration of the munition. NTO is the only component occurring at high enough levels to possibly pick up with the pans or the outer distance sweepings (19–25 m).

Phase 3: Unconfined Charge Distribution Tests

The mass of RDX recovered from each of the 15 steel witness plate segments for the 2.5 g charge was not equal, however the collection segments (areas) along the length of the X axis had a consistently higher concentration of residue (Figure 4b). The residue from the 5 g charge appears to be more evenly distributed across the plate, with similar deposits of residue on each collection segment (Figure 4c). However, for both charge sizes, the residue has traveled further than predicted by the ProSAir tool, which was confirmed by detection of higher than predicted residue mas at the boundry of the witness plate. Residues were also detected (but not measured) beyond the witness plates.

4 Discussion

Field research on high-order detonation residues dispersal indicates that uniform radial distribution of particles rarely

Figure 6. Radial high-order particle distribution.

⤢⤢ These are not the final page numbers!

Table 6. High-order Detonation Particle Spatial Distribution (All particles)

Test	Distance	Annular Area (m²)	Mass[c] (mg/%)	>2 mm (mg/#)	1–2 mm (mg/#)	0.6–1 mm (mg/#)	0.25–0.6 mm (mg/#)	<0.25 mm² (mg/%)[d]
HI-1	0–4 m	50	69/19	0/0	7/2	1/8	8/350	53/77
Pans	4–5 m	28	81/23	0/0	2/4	7/50	12/300[1]	60/74
	5–6 m	35	86/24	0/0	12/3	1/7	9/200[1]	64/74
	6–7 m	41	46/13	0/0	<1/1	1/10	4/90	41/89
	7–8 m	47	40/11	0/0	1/2	3/7	6/100[1]	30/75
	8–9 m	53	22/6	1/1	0/0	1/3	1/110	19/86
	9–10 m	60	12/3	0/0	0/0	1/3	1/40	10/83
	Totals	314	356 mg	1/1	22/12	15/88	41/1200	280 mg
	Means		51 mg	–/–	3/2	2/13	6/170	40/80
HI-1	19–20 m	123	1300/42	260 /12	190/30	52/35	120/300[1]	690/53
All	20–21 m	129	550/18	0/0	190/36	23/29	39/300[1]	300/55
	21–22 m	135	370/12	0/0	89/18	17/13	33/100[1]	230/62
	22–23 m	141	480/15	0/0	69/12	17/34	50/1000[1]	340/71
	23–24 m	148	220/7	0/0	5/5	16/14	14/200[1]	180/82
	24–25 m	154	140/5	0/0	47/10	9/14	10/200[1]	74/53
	Totals	830	3100 mg	260/12	590/100	130/140	270/2100[1]	1800 mg
	Means		520 mg	43/2	98/16	22/23	45/350[1]	300/58
				>0.6 mm (mg/#)	0.25–0.6 mm (mg/#)	0.12–0.25 mm (mg/#)	<0.12 mm² (mg/%)	
HI-2	2–3 m	16	1/2	<1/3	<1/20	<1/220	1/>99	
Pans 0-10m)	3–4 m	22	2/3	<1/5	<1/100	<1/500[1]	1/50	
	4–5 m	28	6/10	<1/1	<1/32	<1/120	6/>99	
	5–6 m	35	10/17	<1/4	<1/42	<1/450[1]	9/90	
	6–7 m	41	10/17	<1/1	<1/2	<1/60	9/90	
	7–8 m	47	9/16	<1/1	<1/60	0/0	8/89	
	8–9 m	53	10/17	<1/4	<1/24	<1/15	10/>99	
	9–10 m	60	10/17	3/3	<1/4	<1/20	8/80	
	Totals	302	58 mg	≈5/19	≈4/36	≈4/170	52 mg	
	Means		7.3 mg	≈0.6/2	≈0.5/5	≈0.5/21	6.5/89	

[a] Estimate based on partial count of particles; [b] Rough order of magnitude estimate is in the thousands of particles (Particles were clumped together); [c] Total mass of particles following measurement; [d] Because of the very large number of particles, a percentage of the total mass in the annulus is given rather than the number of particles <0.25 mm.

Table 7. Estimated Total Detonation Residues

Test	RDX (mg)	DNAN (mg)	NTO (mg)	Overall Efficiency
HI-1	7.8 (0.006 %)[a]	32 (0.013 %)	720 (0.17 %)	99.91 %
HI-3	0.4 (<0.001 %)	1.2 (<0.001 %)	730 (0.17 %)	99.91 %
Prior Tests	7.7 (0.006 %)	7.9 (0.003 %)	540 (0.13 %)	99.93 %

[a] Percent of the original mass of the analyte listed in the column header (%)

Figure 7. Wind-influenced dispersion of dark high-order detonation residues.

occurs. The very small size of the particles, both energetic and metallic, makes them very susceptible to directional dispersal effects of atmospheric conditions, especially wind. The dispersal patterns for the high-order detonations shown in Figure 1 are near ideal. Wind, thermodynamic effects of the detonation fireball, and detonation kinetics all affect the dispersal of residues, resulting in non-uniform distribution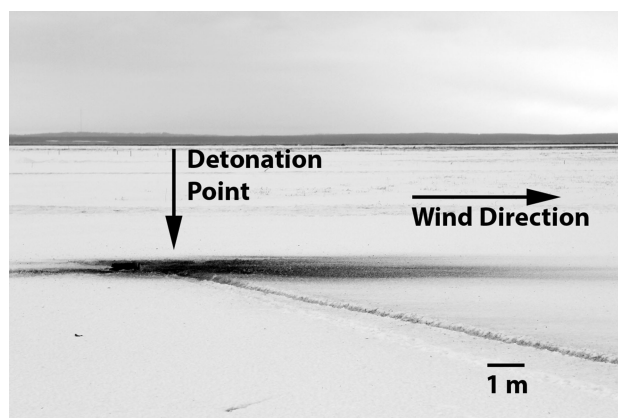 of the particles (Figure 7). Crater (detonation point) residues also tend to be low for live-fired rounds, resulting in areas of up to 10 m² at the detonation point without any detectable energetics [5, 42]. Sampling of residues

M. R. Walsh, T. Temple, M. F. Bigl, S. F. Tshabalala, N. Mai, M. Ladyman

within concentric areas centered on detonation points does show a consistently decreasing deposition amount as the distance increases, but there will be great variability within each concentric area in the mass density of residues due primarily of transport by wind.

The particle dispersion data from the command-detonated mortar rounds further substantiates the non-homogeneous nature of residues deposition from high-order detonations. For our tests, the mass deposition peaks around 5–6 m from the detonation point, demonstrating that proximity to the crater does not necessarily correlate with maximum energetics residues deposition. The residues mass feathers out as distance increased beyond 6 m, as most models would predict. However, the mass of energetics did not peak until more than 20 m from the detonation point, where the mass of NTO residues rapidly rose and then fell. It would be interesting to repeat this test with different size rounds and with swept annuli rather than small pans to get a better indication of particle distribution.

The series of tests conducted at Cranfield University with unconfined charges were designed using maximum residue distribution distances predicted by ProSAir [33]. The results are inconsistent, which may be due to the hand-molding of the PE7 charges or the small critical diameter of the charge size relative to the detonator. The orientation of the suspended charge relative to the witness plates may also not have been accurately reproduced. Therefore, for this experiment, all of these issues could be contributing factors to the ProSAir computational tool prediction not accurately reflecting the maximum distance that the explosive residue could travel. Although the tool gave a useful rough estimate of the maximum mass distribution radius, the Cranfield research demonstrates that further fieldwork is required to generate the empirical data needed to fine tune currently used models.

Most rounds fired into impact ranges function properly, detonating high order. Past research indicates that high-order detonations of conventional munitions contribute only a small amount of energetics contamination on ranges [23]. A single low-order detonation will result in four to five orders of magnitude more energetic residues than a high-order detonation, thus dominating energetics sources on military training ranges [1,3,23]. The very fine residues from high-order detonations are subject to quick dissolution because of a high surface area to mass ratio, a condition that will lead to a high-concentration slug of energetics moving through the soil column [43]. However, the very small amount of energetic material contained in the residues is more easily attenuated by natural processes and may not be a significant factor for most compounds. To better characterize and model energetics deposition on training ranges, low-order detonations will need to be addressed, especially for the emerging insensitive munitions with their higher energetics deposition and highly soluble energetic compounds [13–17].

Data from only a few high-order detonation tests are obviously not sufficient to optimize current models, and there is a need to incorporate low-order and partial detonation data into these models as well. More field-testing of munitions needs to be conducted to generate a meaningful empirical database. These data can then be used to modify current models [19]. Finally, tests in Phase 2 and Phase 3 were conducted above smooth surfaces. The very fine residues from the high-order detonations may be skewed away from the detonation points as a result of lateral transport caused by the shock wave and the expanding gases from the detonation. A testing protocol needs to be developed to determine if kinetic transport is a factor in the determination of residues distribution.

5 Conclusions

Energetic particle dispersion from high-order detonations is a complex process that does not lend itself to simple modeling. Many factors affecting particle dispersion are not included in current models. These models have been modified based on available particle dispersion data, but the data are limited and need to be supplemented with additional empirical data. Data presented in this paper on particle dispersion areas, distance-related mass deposition data, and mass deposition based on perceived density of residues deposition can all be used to further refine modeling of high-order detonation deposition of energetics. Particle counts and mass of energetics based on radial distances from detonation are presented that will also assist in refining dispersion models. Previous research indicates that low-order detonations contribute most of the energetics readily available on ranges, thus residues data from these detonations must be incorporated in models to make them relevant for predicting environmental impacts on training ranges from live-fire munitions.

List of Acronyms

AP   Ammonium Perchlorate (NH_4ClO4)
BIP   Blow in Place
C4   Composition C-4 (91 % RDX)
Comp B   Composition B explosive (59.5 % RDX, 39.4 % TNT)
CRREL   Cold Regions Research and Engineering Laboratory
DNAN   Dinitroanisole ($C_7H_6N_2O_5$)
HO   High Order
HPLC   High Performance Liquid Chromatography
IHE   Insensitive High Explosive
IM   Insensitive Munition
IMX   IM Explosive
ISO   International Standards Organization
LC-PDA   Liquid Chromatography – Photo-Diode Array
LO   Low Order
NATO   North Atlantic Treaty Organization

↖↖ These are not the final page numbers!

NTO   Nitrotriasolone ($C_2H_2N_4O_3$)
NQ   Nitroguanidine ($CH_4N_4O_2$)
PETN   Pentaerythritol-tetranitrate ($C_5H_8N_4O_{12}$)
ProSAir Propagation of Shock in Air (Modeling software)
RDX   Hexogen (($O_2NNCH_2)_3$)
TNT   Trinitroluene ($C_7H_5N_3O_6$)

Acknowledgements

References

[1] T. F. Jenkins, A. D. Hewitt, C. L. Grant, S. Thiboutot, G. Ampleman, M. E. Walsh, T. A. Ranney, C. A. Ramsey, A. J. Palazzo, J. C. Pennington, Identity and Distribution of Residues of Energetic Compounds at Army Live-fire Training Ranges, *Chemosphere* **2006**, *63*, 1280–1290.

[2] J. D. Kelleher, Explosive Residue: Origin and Distribution, in *Forensic Science Communications*, **2002** Vol. 4, No. 2, April 2002. US Federal Bureau of Investigation, Washington, DC, USA. Available from: http://www.fbi.gov/about-us/lab/forensic-science-communications/fsc/april2002/kelleher.htm. [Accessed July **2016**]

[3] L. Pichtel, Distribution and Fate of Military Explosives and Propellants in Soil: A review, *Appl. Environ. Soil Sci.* **2012**, Article ID 617236, 33 pages. doi:10.1155/2012/617236.

[4] S. Thiboutot, G. Ampleman, S. Brochu, E. Diaz, R. Martel, J. Hawari, G. Sunahara, M. R. Walsh, M. E. Walsh, Canadian Programme on the Environmental Impacts of Munitions, *1st European Conference on Defence and the Environment*, Helsinki, Finland **2013**.

[5] A. D. Hewitt, T. F. Jenkins, M. E. Walsh, M. R. Walsh, S. Taylor, RDX and TNT Residues from Live-fire and Blow-in-place Detonations, *Chemosphere* **2005**, *61*, 888–894.

[6] M. R. Walsh, M. E. Walsh, A. D. Hewitt, Energetic Residues from Field Disposal of Gun Propellants, *J. Hazard. Mater.* **2010**, *173*, 115–122.

[7] M. R. Walsh, M. E. Walsh, Ø. A. Voie, Presence and Persistence of White Phosphorus on Military Training Ranges, *Propellants Explos. Pyrotech.* **2014**, *39(6)*, 922–931.

[8] M. E. Walsh, M. R. Walsh, C. M. Collins, C. H. Racine, White Phosphorus Contamination of an Active Army Training Range. *Water Air Soil Pollut.* **2014**, *225*, 2001 (doi:10.1007/s11270-014-2001-2).

[9] J. H. Lever, S. Taylor, L. Perovich, K. Bjella, B. Packer, Dissolution of Composition-B Detonation Residuals, *Environ. Sci. Technol.* **2005**, *39*, 8803–8811.

[10] M. E. Walsh, S- Taylor, A. D. Hewitt, M. R. Walsh, C. A. Ramsey, C. M. Collins, Field observations of the persistence of Comp B

[11] C. H. Racine, M. E. Walsh, B. D. Roebuck, C. M. Collins, D. J. Calkins, L. R. Reitsma, P. J. Buchli, G. Goldfarb, White Phosphorus Poisoning of Waterfowl in an Alaskan Salt Marsh, *J. Wildl. Dis.* **1992**, *28(4)*, 669–673.

[12] J. Clausen, D. Robb, D. Curry, N. Korte, A Case Study of Contaminants on Military Ranges: Camp Edwards, Massachusetts, USA, *Environ. Pollut.* **2004**, *129*, 13–21.

[13] M. R. Walsh, M. E. Walsh, S Taylor, C. A. Ramsey, D. B. Ringelberg. Characterization of PAX-21 insensitive Munitions Detonation Residues, *Propellants Explos. Pyrotech.* **2013**, *38*, 399–409.

[14] M. E. Walsh, M. R. Walsh, S. Taylor, C. A. Ramsey, Deposition of DNAN and RDX from PAX-21 and IMX-104 Detonations, *Proceedings of the JANNAF Workshop on Insensitive Munitions* **2014**, 23–31.

[15] M. R. Walsh, M. E. Walsh, C. A. Ramsey, S. Thiboutot, G. Ampleman, E. Diaz, J. E. Zufelt, Energetic Residues from the Detonation of IMX-104 Insensitive Munitions, *Propellants Explos. Pyrotech.* **2014**, *38(2)*, 243–250.

[16] S. Taylor S, D. B. Ringelberg, K. Dontsova, C. Daghlian, M. E. Walsh, M. R. Walsh, Insights into the Dissolution and the Three-dimensional Structure of Insensitive Munitions Formulations, *Chemosphere* **2013**, *93*, 1782–1788.

[17] M. R. Walsh, M. E. Walsh, C. A. Ramsey, S. Brochu, S. Thiboutot, G. Ampleman, Perchlorate Contamination from the Detonation of Insensitive High-explosive Rounds, *J. Hazard. Mater.* **2013**, *262*, 228–233.

[18] SERDP/ESTCP. *Environmental Restoration Program: Range Contamination.* Found at: https://www.serdp-estcp.org/Program-Areas/Environmental-Restoration/Contaminants-on-Ranges (Accessed 12 JUL **2016**).

[19] J. E. Hathaway, J. P. Rishel, M. E. Walsh, M. R. Walsh, S. Taylor, Explosive Particle Soil Surface Dispersion Model for Detonated Military Munitions, *Environ. Monit. Assess.* **2015**, *187(7)*, 1–15.

[20] P. E. Montanaro, *TRAJ – A Two-dimensional Trajectory Program for Personal Computers*, Naval Surface Warfare Center, Washington, DC **1990**.

[21] M. M. Crull, *Prediction of Primary Fragmentation Characteristics of Cased Munitions*, USAESC Report No. 500203, U.S. Army Engineering & Support Center, Huntsville, AL USA **1998**.

[22] Interstate Technology and Regulatory Council (ITRC). *Incremental Sampling Methodology: Representative Sampling, Confident Decisions.* **2011** Found at: www.itrcweb.org/ism-1. (Accessed 12 JUL **2016**).

[23] M. R. Walsh, M. E. Walsh, I Poulin, S Taylor, T. A. Douglas, Energetic Residues from the Detonation of Common US Ordnance, *Int. J. Energ. Mater. Chem. Propul.* **2011**, *10(2)*, 169–186.

[24] M. R. Walsh, M. E. Walsh, G. Ampleman, S. Thiboutot, S. Brochu, T. F. Jenkins, Munitions Propellants Residue Deposition Rates on Military Training Ranges, *Propellants Explos. Pyrotech.* **2012**, *37(4)*, 393–406.

[25] S. Taylor, A. D. Hewitt, J. H. Lever, C. Hayes, L. Perovich, P. Thorn, C. Daghlian, TNT Particle Size Distributions from Detonated 155-mm Howitzer Rounds, *Chemosphere* **2004**, *55*, 357–367.

[26] H. J. Yallop, *Explosion Investigation*, Forensic Science Society, Harrogate, North Yorkshire, UK **1980**.

[27] M. R. Walsh, M. E. Walsh, C. A. Ramsey, R. J. Rachow, J. E. Zufelt, C. M. Collins, A. B. Gelvin, N. M. Perron, S. P. Saari, *Energetic Residues Deposition from 60-mm and 81-mm Mortars*, ERDC/CRREL Technical Report TR-06-10. US Army Cold Regions Research

and Engineering Laboratory (USA CRREL), Hanover, NH USA **2006**.

[28] L. Dauphine, C. Doyle, *USACE Report of Findings for Study of Ammunition Dud and Low-order Detonation Rates*, USAEC Report SFIM-AEC-ET-CR-200049. US Army Environmental Center (USAEC), Aberdeen Proving Ground, MD **2000**.

[29] L. Dauphine, C. Doyle, *USACE Report of Findings for Phase II Study of Ammunition Dud and Low-order Detonation Rates*, USAEC Report SFIM-AEC-PC-CR-200139, USAEC, Aberdeen Proving Ground, MD **2001**.

[30] R. H. Bishop, *Maximum Missile Ranges from Cased Explosive Charges*, SNL Report No. SC-4205 (TR). Sandia National Laboratories (SNL), Albuquerque, New Mexico, USA **1958**.

[31] J. E. Kennedy, *Gurney Energy of Explosives: Estimation of the Velocity and Impulse Imparted to Driven Metal*, SNL Report No. SC-RR-70-90. Sandia National Laboratory, Albuquerque, NM **1970**.

[32] N. Abdul-Karim, R. Morgan, R. Binions, T. Temple, K. Harrison, The Spatial Distribution of Post-blast RDX Residue: Forensic Implications, *J. Forensic Sci.* **2013**, *58(2)2*, 365–371 (DOI: 10.1111/1556-4029.12045).

[33] G. Lindkvist, S. A. Forth, *ProSAir Computational Blast Loading Tool*, Cranfield University, Shrivenham, UK. **2016**. Available from: http://www.cranfield.ac.uk/facilities/cds-prosair-computational-blast-loading-tool (Accessed 12 JUL **2016**).

[34] T. F. Jenkins, M. E. Walsh, P. H. Miyares, A. D. Hewitt, N. H. Collins, T. A. Ranney, Evaluation of the Use of Snow-covered Ranges to Estimate the Explosives Residues that Result from High Order Detonations of Army Munitions, *Thermochim. Acta* **2002**, *384*, 173–185.

[35] M. R. Walsh, M. E. Walsh, C. A. Ramsey, Measuring Energetic Contaminant Deposition Rates on Snow, *Water Air Soil Pollut.* **2012**, *223*, 3689–3699.

[36] M. R. Walsh, M. E. Walsh, C. A. Ramsey, T. F. Jenkins, An Examination of Protocols for the Collection of Munitions-derived Ex-

plosives Residue on Snow-covered Ice, ERDC/CRREL Technical Report TR-05-8. USA CRREL, Hanover, NH USA **2005**.

[37] North Atlantic Treaty Organization, *Guidance on the Assessment and Development of Insensitive Munitions*, NATO Standardization Agency, Defence Investment Division, Allied Ordnance Publication AOP-39, pp. I-1 to I-4. NATO Standardization Organization, Brussels, Belgium **2010**.

[38] US Department of Defense (US DoD), *Hazard Assessment Tests for Non-nuclear Munitions (14 JUL 2003 update)*, US DoD Test Method Standard MIL-STD-2105C, pp 7–8. US Department of Defense, Washington, DC **1994**.

[39] M. E. Walsh, Analytical Methods for Insensitive High Explosives, *J Energ. Mater.* **2016**, *34*, 76–91.

[40] USEPA, *Nitroaromatics and Nitramines by High-Pressure Liquid Chromatography*, EPA SW846 Method 8330B, US Department of Environmental Protection, Washington, DC, USA, **2006** (Accessed May **2013**): (http://www.epa.gov/osw/hazard/testmethods/pdfs/8330b.pdf).

[41] M. R. Walsh, *Energetics Residues from the Detonations of IMX-101 and IMX-104 Munitions*, ERDC/CRREL Test Report (Distribution limited). USA CRREL, Hanover, NH USA **2016**.

[42] A. D. Hewitt, T. F. Jenkins, T. A. Ranney, J. A. Stark, M. E. Walsh, S. Taylor, M. R. Walsh, D. J. Lambert, N. M. Perron, N. H. Collins, R. Karn. *Estimates for Exploisves Residue from the Detonation of Army Munitions*, ERDC/CRREL Technical Report TR-03-16. USA CRREL, Hanover, NH USA **2003**.

[43] S. Taylor, J. H. Lever, J. Fadden, N. Perron, B. Packer. Simulated Rainfall-driven Dissolution of TNT, Tritonal, Comp B, and Octol Particles, *Chemosphere* **2009**, *75*, 1074–1081.

↖↖ These are not the final page numbers!

FULL PAPER

M. R. Walsh*, T. Temple, M. F. Bigl, S. F. Tshabalala, N. Mai, M. Ladyman

1 – 11

Investigation of Energetic Particle Distribution from High-Order Detonations of Munitions